Progress In Electromagnetics Research C, Vol. 103, 59–70, 2020

Dual Band-Notched UWB Antenna with Improved Radiation Pattern

Junhui Wang*

Abstract—In this paper, a novel microstrip-fed compact antenna with dual band-notched characteristic is presented for ultra-wideband (UWB) applications. Assisted with symmetrical open-circuited stubs, a UWB impedance matching can be achieved. A novel modified capacitively loaded loop (CLL) resonator is proposed to realize the dual notched bands. By symmetrically placing a couple of proposed resonators in the vicinity of the feed line, dual band-notched properties in 3.4–3.7 GHz for WiMAX and 5.15–5.825 GHz for WLAN are generated. The good performance of the dual notched bands, stable gain, and radiation patterns in the operating bands make the proposed antenna a good candidate for various UWB applications.

1. INTRODUCTION

Since the Federal Communication Commission (FCC) released the frequency band 3.1–10.6 GHz for commercial ultra-wideband (UWB) systems, both industry and academia have conducted tremendous efforts on the UWB radio technology [1]. Planar monopole antennas, as one of the most attractive candidates for UWB antennas, have recently been paid more attention due to their small size and easy integration. Although this type of antenna can be matched over the entire UWB bandwidth with ease, there are still many challenges to face for the UWB applications. One of the main issues is the radiation pattern degradation of the antenna at high frequencies. This deterioration may cause mistake or distortion in some applications which require a stable radiation pattern [2]. Another significant challenge is to avoid electromagnetic interference with other existing narrowband services which occupy some of the spectra in the UWB, such as 3.4–3.7 GHz for Worldwide Interoperability for Microwave Access (WiMAX) service and 5.15–5.35 & 5.725–5.825 GHz for Wireless Local Area Network (WLAN) service. Therefore, a dual band-notched UWB antenna with a stable radiation pattern is desirable.

Until now, several techniques have been proposed to improve the radiation pattern of UWB antennas [2–7]. However, most of these antennas have large dimensions or bulky volumes [2, 3, 5, 6]. For a conventional circular monopole antenna, the radiation patterns at high frequencies are distorted due to the undesired current problem, this paper presents a novel microstrip-fed UWB antenna, which mainly comprises a small circular patch and a modified ground plane. A pair of symmetrical parallel stubs are extended from the ground plane to improve the impedance matching at the low-frequency stage. It should be noted that the radius of the circular patch is much smaller than that of a conventional monopole antenna [8]. Assisted with the pair of extended stubs and the small circular patch, the radiation patterns of the proposed antenna can be improved at the high-frequency stage.

In this paper, a novel microstrip-fed planar UWB antenna with dual notched bands is proposed. A pair of symmetrical open-circuited stubs are extended from the ground plane to achieve good impedance matching at low frequencies. To realize the dual band-notched characteristics, a novel modified capacitively loaded loop (CLL) resonator is introduced, which is different from the conventional

Received 19 March 2020, Accepted 4 June 2020, Scheduled 18 June 2020
* Corresponding author: Junhui Wang (xidian_wjh@163.com).
The author is with the Southwest China Institute of Electronic Technology, Chengdu 610036, China.

approach [9–14]. By adjusting the dimension of the modified CLL resonator, we can easily obtain the desired notched bands to avoid interferences. Moreover, except for the notched bands, the proposed antenna exhibits excellent performance of VSWR in the entire operating band. The proposed design is simulated using the ANSYS High Frequency Structure Simulator (HFSS), one commercial 3-D full-wave electromagnetic simulation software. The antenna prototype is fabricated and measured to demonstrate the feasibility of the proposed design strategy.

2. ANTENNA CONFIGURATION

Figure 1 shows the proposed dual band-notched monopole antenna which mainly comprises a circular-shape radiation patch, a partially modified ground plane with two extended open-circuited stubs, and a couple of symmetrical modified CLL elements. In order to enhance the impedance bandwidth, especially in the low frequency band, a pair of symmetrical stubs are extended from the ground plane. The proposed antenna is fed by a microstrip line and printed on an FR4 substrate with a thickness of 40 mil, relative dielectric constant of 4.4, and loss tangent of 0.02. The width of the microstrip feed line is chosen as 1.86 mm to achieve the characteristic impedance of 50 Ω. The width of the upper section of the feed line tapers from 1.86 to 1 mm for good impedance matching. To achieve the dual band-notched characteristic, a couple of modified CLL resonators are symmetrically placed near the feed line to generate notched bands with central frequencies of 3.5 and 5.5 GHz. Based on the optimized dimensions given in Table 1, a prototype of dual-band-notched antenna for UWB applications is designed and fabricated. Fig. 2 presents a photograph of the constructed antenna.

Table 1. Optimized antenna parameters.

Parameter	W	H	R	l_e	w_e	g	w_f	w_{ft}
Values (mm)	26	33	4.8	21	0.5	1	1.86	1
Parameter	l_{ft}	r_c	w_l	w_h	l_c	w_s	S	
Values (mm)	4	3.5	0.3	0.8	1.5	1	3.35	

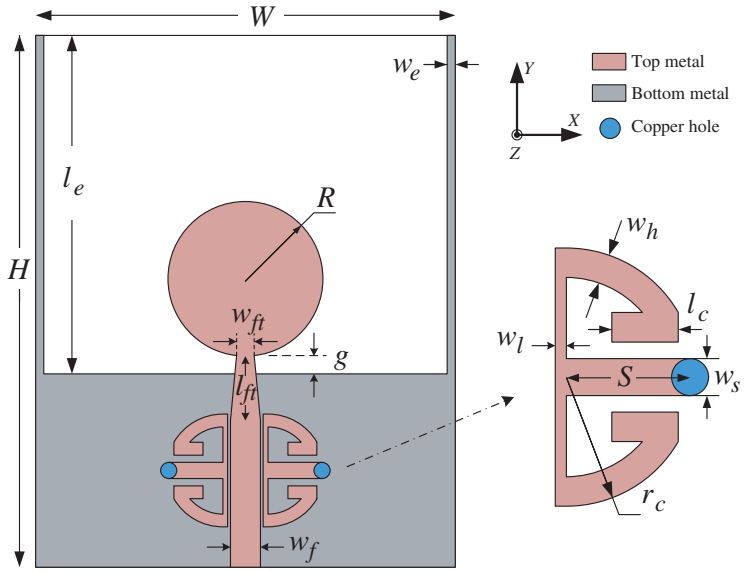

Figure 1. Geometry of the proposed antenna.

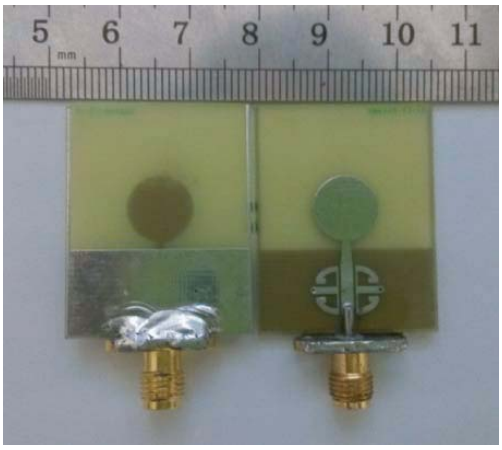

Figure 2. Prototype of the proposed antenna.

3. ANTENNA DESIGN AND ANALYSIS

3.1. UWB Antenna with Improved Radiation Pattern

Figure 3 shows a representative conventional circular monopole antenna, for which the first resonance of the antenna is associated with the circular dimension [8]. To fulfill the entire UWB, the circular patch radius is always chosen as quarter wavelength at 3.5 GHz. However, it can be seen from Fig. 4 that the radiation pattern is distorted in the high frequency band, especially at frequencies above 9 GHz, and a null even appears in the main broadside direction (Z-axis) at 11 GHz, which might cause the transmission distortion to some extent.

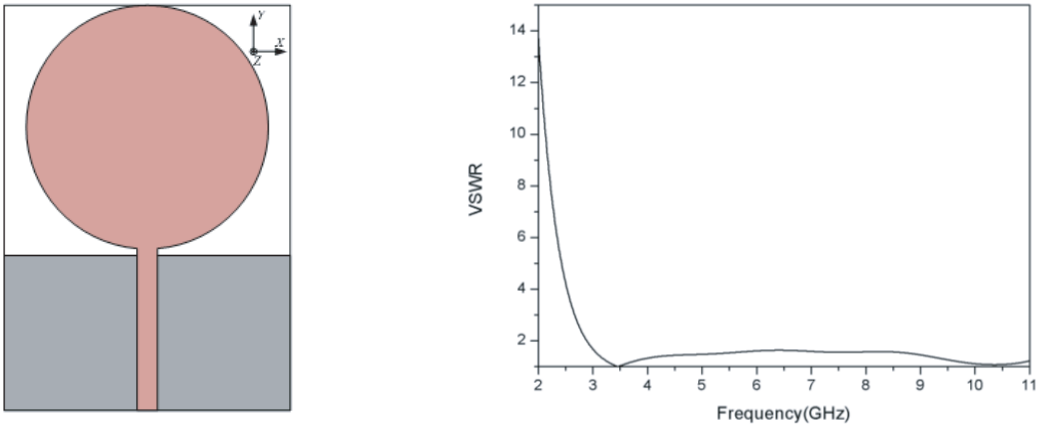

Figure 3. The representative circular monopole antenna.

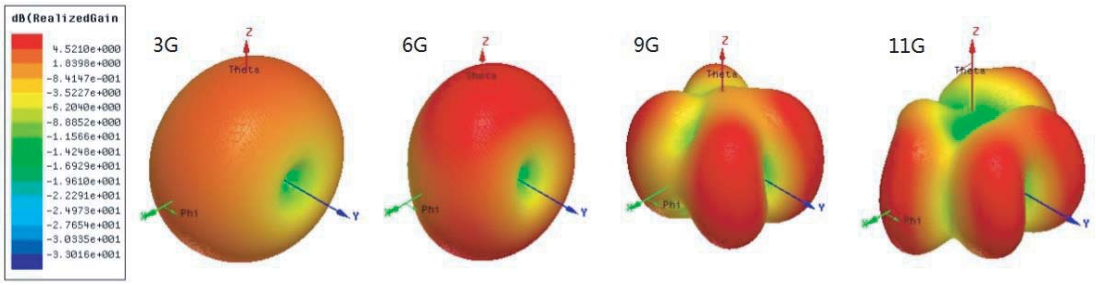

Figure 4. The 3-D radiation pattern at different frequencies for the conventional monopole antenna.

The cause for the deformation of the far-field radiation pattern has been added in the revised paper. Fig. 5 and Fig. 6 show the surface current vector at 9 and 11 GHz for the traditional UWB patch antenna. It can be seen that the current is bidirectional whether in the circular patch or in the rectangular ground, which means that the radiated far-field would cancel in the $\pm Z$ direction and finally result in the deformation in the radiation pattern at 9 and 11 GHz. It should be noted that the strong current intensity on the feedline does not contribute to the radiation due to the opposite current direction on the corresponding ground area underneath the feedline.

In order to improve the radiation pattern at high frequencies, a novel planar UWB antenna, which mainly comprises a small circular patch and a modified ground plane with two symmetric stubs, is presented in this paper. The diameter of the circular patch is only about 4.8 mm, which is about one fifth the size of the previously mentioned conventional patch. As shown in Fig. 7, it should be noted that the impedance matching will become worse with smaller patch size than the fifth of the traditional patch size. Moreover, as can be seen from Fig. 8, the realized gain pattern of the presented antenna will also deteriorate with smaller patch size.

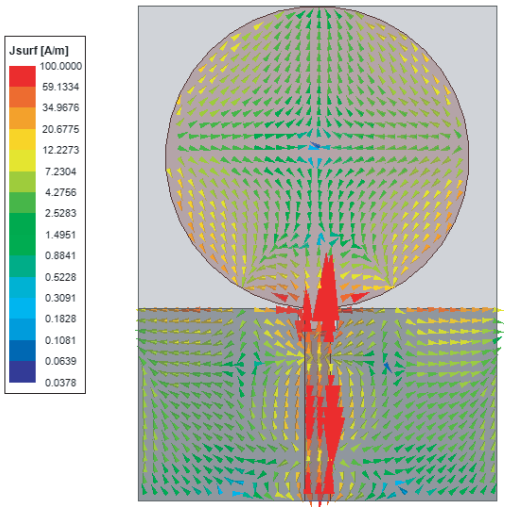

Figure 5. The surface current vector at 9 GHz for the traditional UWB antenna.

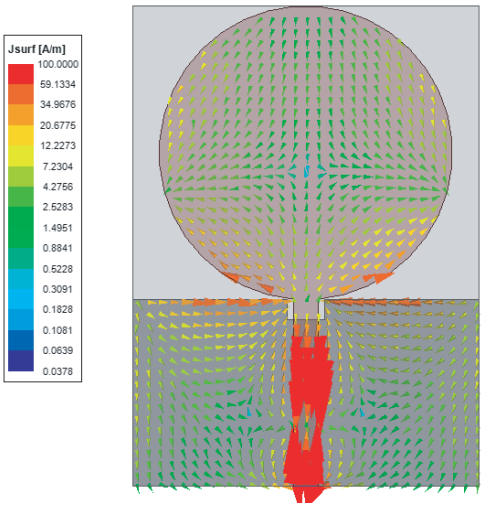

Figure 6. The surface current vector at 11 GHz for the traditional UWB antenna.

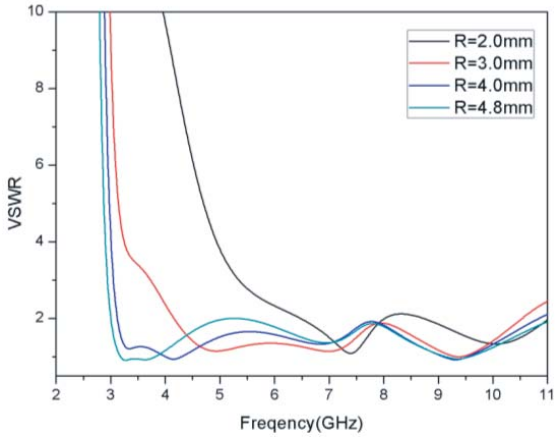

Figure 7. The VSWR for the presented antenna with different circular patch radius.

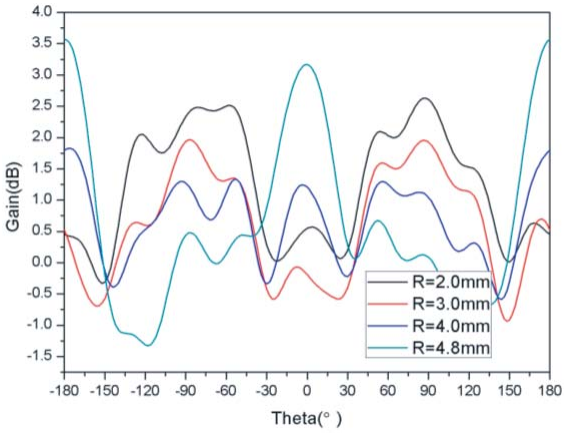

Figure 8. The XOZ-plane gain pattern for the presented antenna with various patch radius.

By employing the two extended open-circuited stubs, the radiation pattern at high frequencies can be greatly improved. The surface current distributions of the presented antenna at 9 and 11 GHz are shown in Fig. 9 and Fig. 10. It can be seen that compared with the current distribution in Fig. 5 and Fig. 6 for the traditional UWB antenna, the current distributions in the patch and ground are greatly changed with the help two extended open-circuited stubs. Significant amounts of current in the small circular patch and ground plane have the same direction, which is beneficial for the far-field radiation pattern at high frequencies, and the main beam of the radiation pattern returns to the broadside direction. Therefore, the proposed UWB antenna exhibits an improved radiation pattern in the high frequency band with the help of the two open-circuited stubs.

Figure 11 shows the simulated 3-D radiation pattern at different frequencies for the proposed antenna. By comparing high-frequency radiation patterns of Fig. 4 and Fig. 11, it can be seen that the radiation pattern at high frequencies can be greatly improved, and the main beam of radiation pattern at 10 GHz returns to Z-axis direction by employing two symmetric extended open-circuited stubs, which means that the proposed UWB antenna exhibits satisfying radiation pattern in the whole operating frequency band.

Another significant function of the pair of extended stubs is to improve the impedance bandwidth

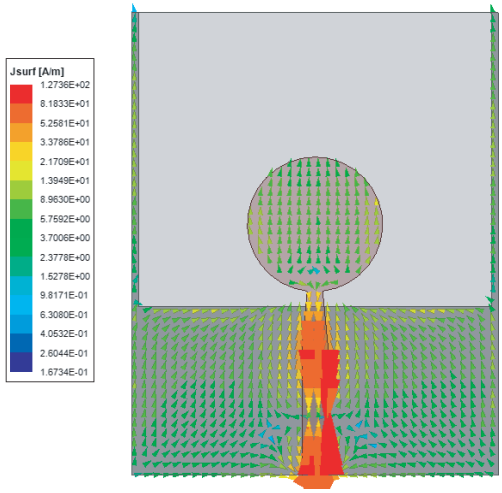

Figure 9. The surface current vector at 9 GHz for the presented UWB antenna.

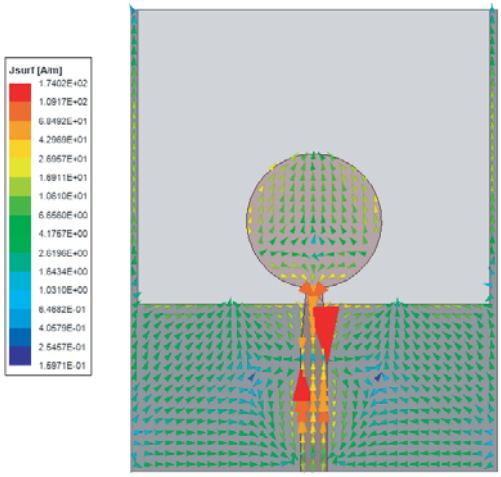

Figure 10. The surface current vector at 11 GHz for the presented UWB antenna.

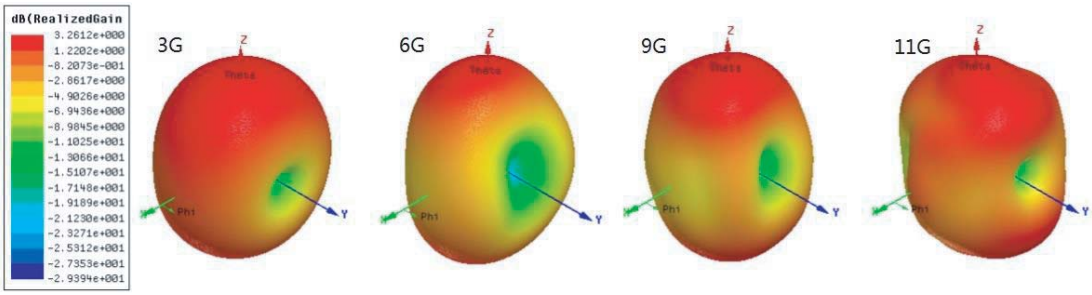

Figure 11. The 3-D radiation pattern at different frequencies for the proposed antenna.

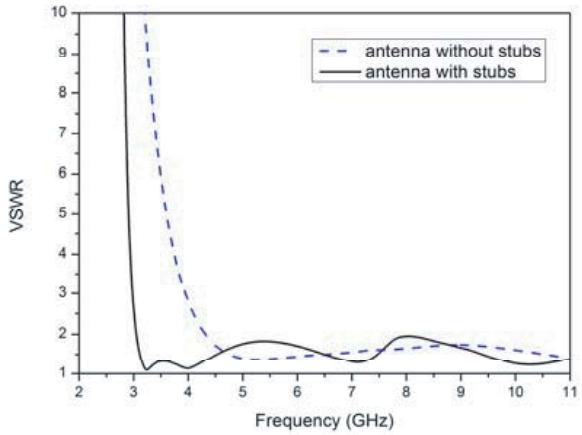

Figure 12. Simulated VSWR results of the antenna with and without stubs.

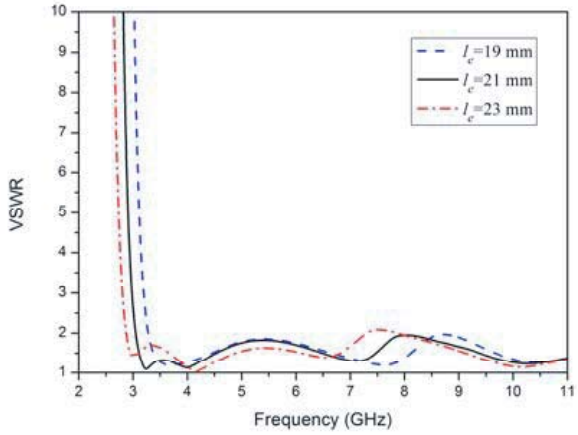

Figure 13. Simulated VSWR results with different lengths l_c of the open-circuited stubs.

at low frequencies. With the addition of the two stubs, a new resonance in the low frequency band is introduced. Fig. 12 shows the simulated VSWR results of the antenna with and without open-circuited stubs. It can be seen that at low frequencies, the impedance matching is greatly improved by introducing the extended stubs. Fig. 13 indicates simulated VSWR results with different lengths L_e of the stubs.

As illustrated in this figure, the edge of low operation frequency decreases as L_e increases. The width of the stubs is not sensitive to the impedance matching in the operation frequency band.

To further explain the performance, the simulated surface current distributions for the antennas with and without open-circuited stubs at 3 GHz are shown in Fig. 14. Comparing the surface currents of the two antennas, it can be seen that the current of the proposed UWB antenna at 3 GHz is mainly concentrated on the two extended stubs. Therefore, the pair of stubs act as two monopoles in low frequency modes, thus the reduced radiation efficiency of the circular radiator at low frequencies will be compensated by the introduced open-circuited stubs.

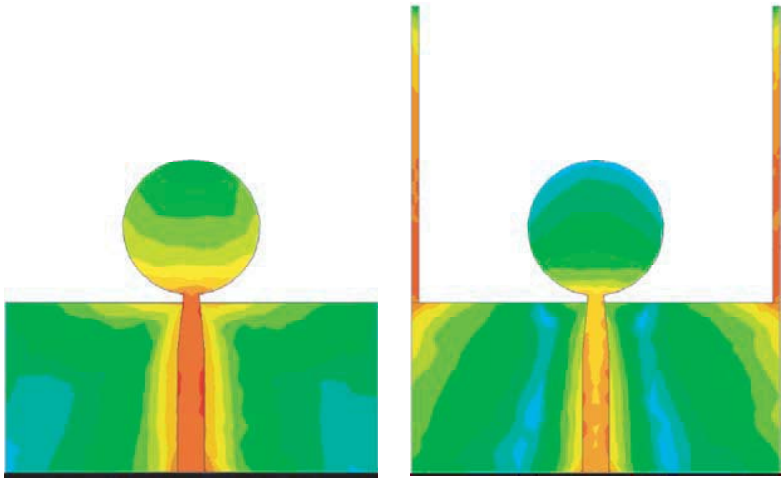

Figure 14. Surface currents distribution of the antenna (a) without and (b) with stubs at 3 GHz.

3.2. Dual-Band Notched UWB Antenna

A novel modified CLL resonator is introduced to achieve the dual notched bands. Fig. 15 shows the evolving process of obtaining the proposed modified CLL structure presented in the paper. Type I is the conventional CLL structure to be used as the notch filter for the UWB antenna. Similar to the split ring resonator (SRR), the conventional CLL resonator is self-resonant and has its loop inductance and cut capacitance. The resonant frequency can be given approximately by the expression [15]

$$f_{notch} = \frac{c}{2L_{CLL} \cdot \sqrt{\varepsilon_{eff}}} \tag{1}$$

where L_{CLL} is the length of the CLL structure. ε_{eff} is an effective dielectric constant, and c is the speed of light. A low-high-low impedance line is adopted in the structure of Type II to increase

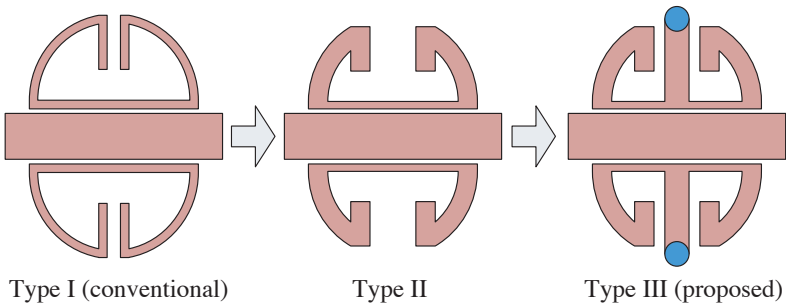

Figure 15. Evolve process of the notch structures.

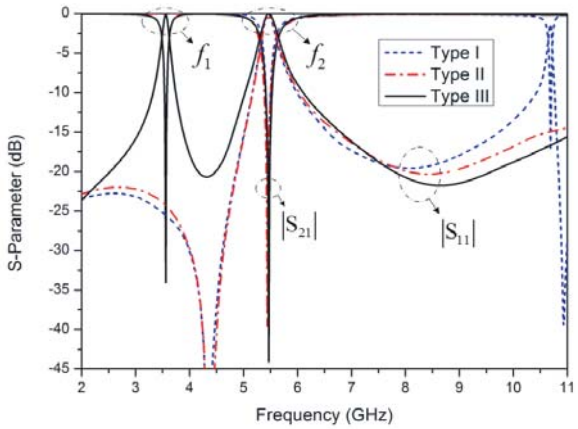

Figure 16. Transfer characteristics of the filter with resonators of Types I, II, and III.

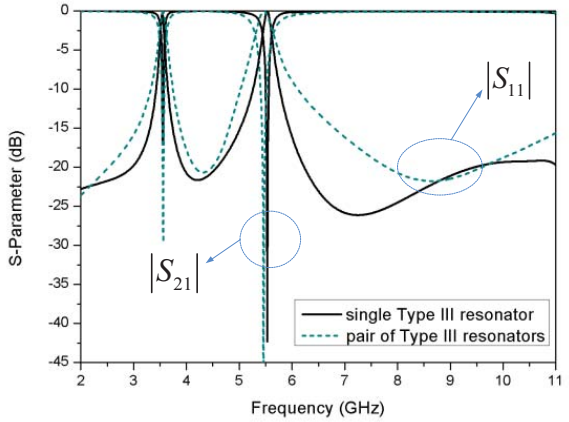

Figure 17. Transfer characteristics of single resonator and pair of Type III resonators.

the harmonic frequency [16], thus improve the impedance matching in the high-frequency band. The proposed structure of Type III is developed from Type II. In the proposed structure (Type III), the middle of the high impedance line is connected to the ground plane through a short line and a via hole.

In order to analyze the frequency response characteristics of the structures shown in Fig. 15, 50 Ω microstrip lines with different types of resonators (Types I, II, and III) are simulated and discussed. Each type of resonators is symmetrically placed near the microstrip line. Fig. 16 shows the simulated results of the two-port filtering structures. All structures are printed on the same substrate with a thickness of 1 mm and relative dielectric constant of 4.4. Identical to the feed line of the antenna, the width of the microstrip line is also chosen as 1.86 mm to achieve the characteristic impedance of 50 Ω. The gap between the microstrip feed line and resonators is fixed at 0.2 mm to ensure proper capacitive coupling.

Comparing the simulated results of Types I and II, it can be seen that the harmonic frequency increases from 10.5 to 13 GHz by employing the low-high-low impedance structure, and thus the impedance matching in the high-frequency band is improved. The simulated results show that Type II displays a single resonant frequency (f_2) at 5.5 GHz within the UWB. In the structure of Type III, the addition of the short-circuited line results in the formation of a new resonance (f_1) at 3.5 GHz, while the other resonance frequency (f_2) remains unchanged. Therefore, the proposed structure (Type III) shows a dual resonance (f_1, f_2) characteristic. It should be noted that only one resonator structure can be used to realize the dual-notched bands. From Fig. 17 it can be seen that compared with the pair of Type III resonators, using single Type III resonator structure can also realize the dual-notched

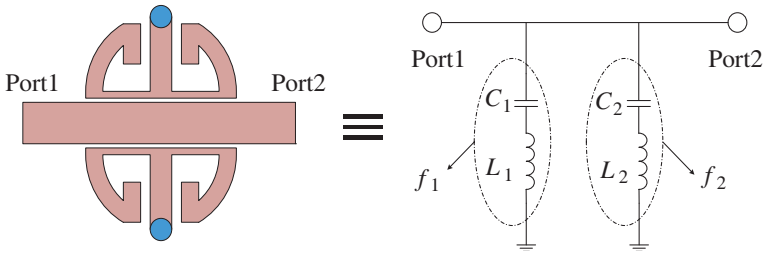

Figure 18. The equivalent circuit of the proposed filter.

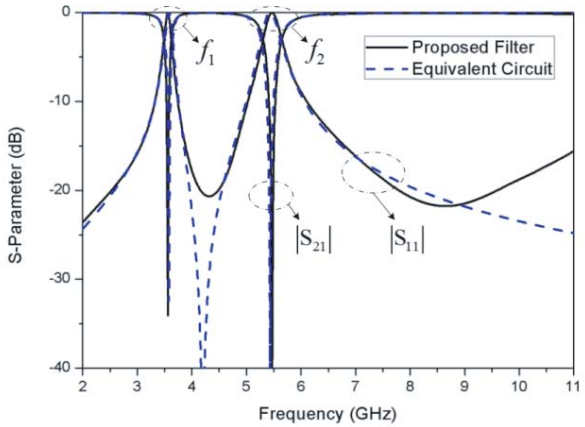

Figure 19. Transfer characteristic of the equivalent circuit.

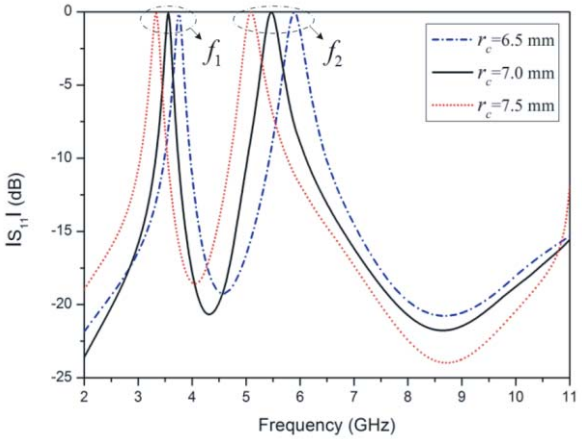

Figure 20. Simulated S_{11} results of the proposed filter in case of different values of r_c.

characteristics with narrower bandwidth. It means that the resonator should be close to the feedline to increase the coupling between them, which may increase the manufacture difficulty due to the extremely small gap.

The proposed Type III structure can be equivalent to two shunt-connected series LC resonance circuit as shown in Fig. 18. Fig. 19 describes the simulated results of the equivalent circuit, while the corresponding parameters of the equivalent lumped components are: $L_1 = 27.50\,\text{nH}$, $C_1 = 0.072\,\text{pF}$, $L_2 = 11.15\,\text{nH}$, $C_2 = 0.077\,\text{pF}$. As to the proposed structure of Type III, the resonant frequency (f_1) structure is mainly determined by the dimensions of the CLL element. Fig. 20 shows the simulated S_{11} results of Type III filter with different values of r_c. It can be seen that the dual resonant frequencies of f_1 and f_2 decrease as r_c increases from 6.5 to 7.5 mm. Fig. 21 indicates the simulated results of Type III according to the variation of length S. From the simulated results, it is found that the resonant frequency f_1 decreases as the length S increases, while the resonant frequency f_2 remains unchanged. As a result, the length S plays an important role in controlling the first resonant frequency f_1. By properly choosing the values of r_c and S, dual desired resonant frequencies can be achieved.

To realize the dual notched bands, a pair of proposed modified CLL resonators (Type III) are symmetrically placed near the feed line of the UWB antenna. Fig. 22 shows the simulated VSWR results against the frequency response for the proposed antenna. The VSWR of the proposed filter (Type III) is also shown for comparison. It is observed that the designed antenna exhibits two notched bands of 3.4–3.7 GHz and 5.15–5.825 GHz. To further explain the performance, the simulated surface currents distributions of the proposed antenna at two resonant frequencies are shown in Fig. 23. As shown in this figure, a significant amount of current at 3.5 GHz is distributed on the vertical line, middle horizontal line, and the via hole of the resonator. It can be found that most of the input signal is coupled from the feed line to the resonators and then flows to the ground plane through the horizontal line and via hole, thus generating the notch resonance at f_1. The current distribution at 5.5 GHz is mainly concentrated on the stepped CLL elements as shown in Fig. 24. The stepped CLL resonators capture

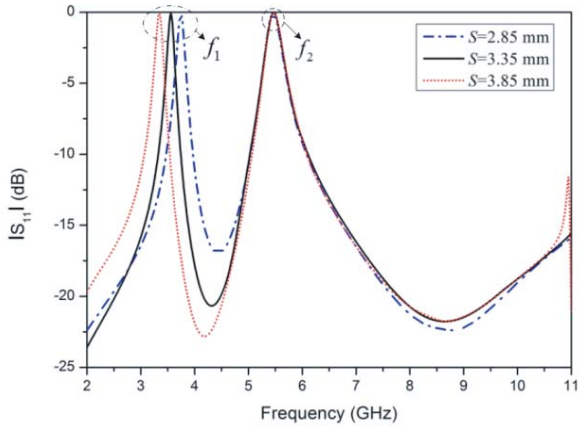

Figure 21. Simulated S_{11} results of the proposed filter in case of different values of S.

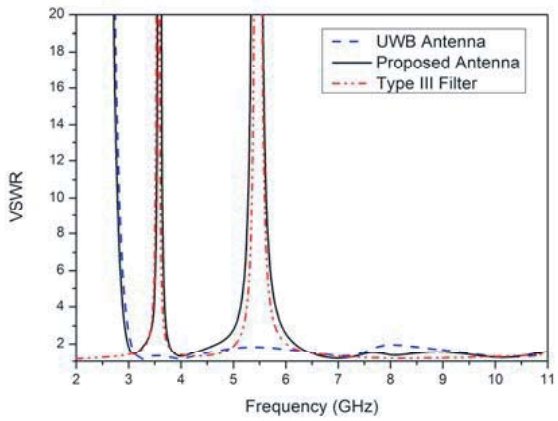

Figure 22. Simulated VSWR results of the proposed antenna and Type III filter.

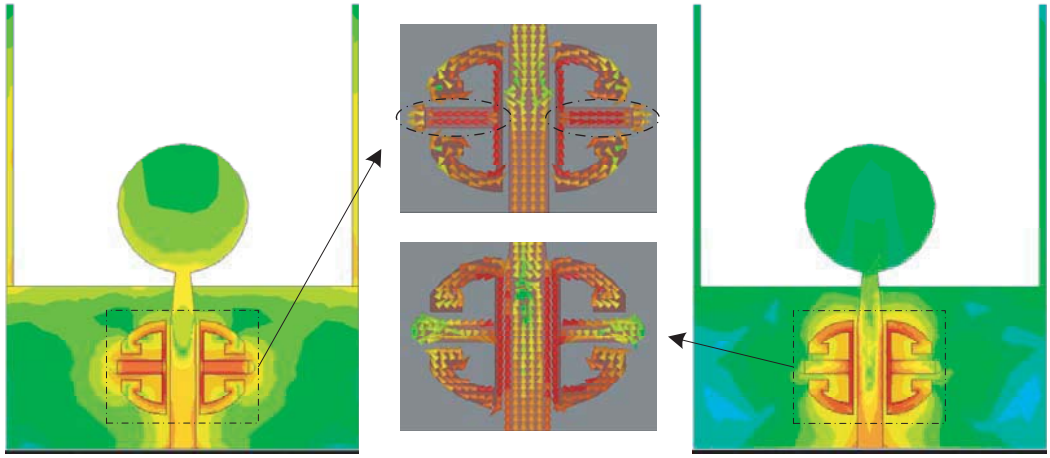

Figure 23. Surface currents distribution of the proposed antenna at (a) 3.5 GHz and (b) 5.5 GHz.

and store most of the input energy at the resonant frequency f_2, which results in another filtering characteristic. Therefore, by employing the proposed modified CLL resonators, the UWB antenna with dual band-notched characteristic is achieved.

4. MEASURED RESULTS AND DISCUSSION

Based on the optimized parameters of the proposed dual band-notched UWB antenna, an antenna prototype is successfully fabricated and measured. Fig. 24 displays the measured and simulated VSWRs for the antenna. The result of the antenna without the notched band is also shown for comparison. It can be observed that the designed antenna exhibits two rejected bands of 3.4–3.7 GHz and 5.15–5.825 GHz, while achieving a wideband performance from 3 to 12 GHz for VSWR < 2. The discrepancy between the measured and simulated results is probably owing to the fluctuation of the dielectric constant and tolerance in manufacturing.

The measured radiation patterns in the E (xy) and H (xz) planes at 3, 4.5, and 9 GHz are plotted in Fig. 25. It can be seen that the proposed antenna has a nearly O-shape radiation pattern in the H-plane and a dipole-like radiation pattern in the E-plane. The measured peak gains and group delay of the designed antenna are shown in Fig. 26. The figure shows that the gains decrease sharply in

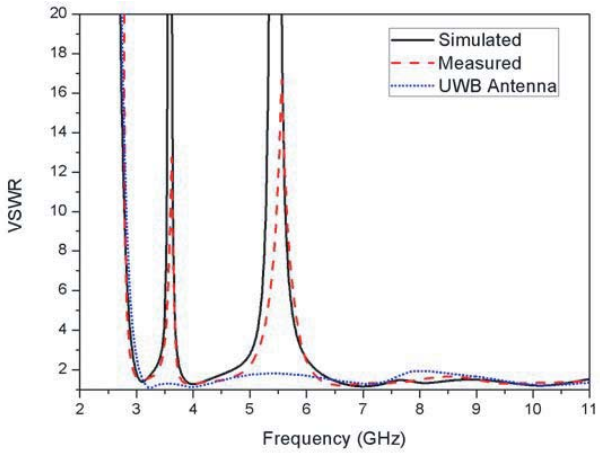

Figure 24. The measured and simulated VSWR results of the proposed antenna.

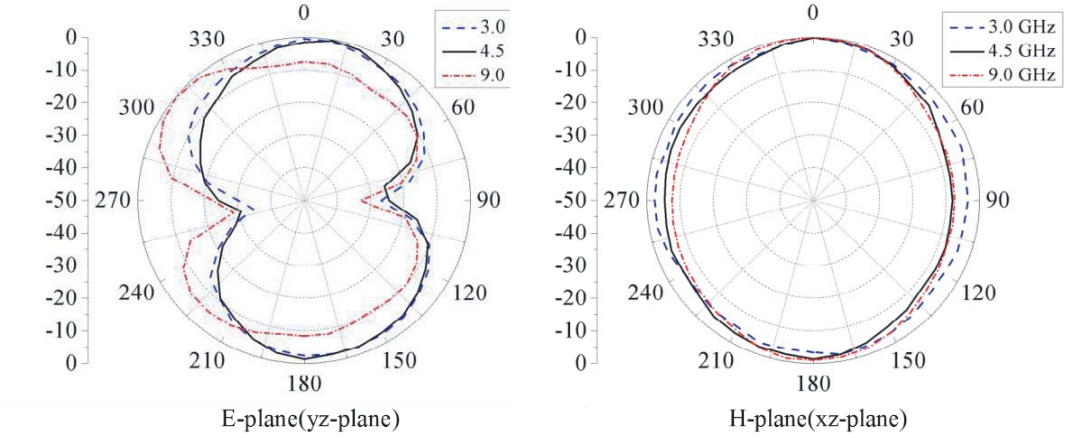

Figure 25. Measured E- and H-plane radiation patterns the proposed antenna at 3, 4.5 and 9 GHz.

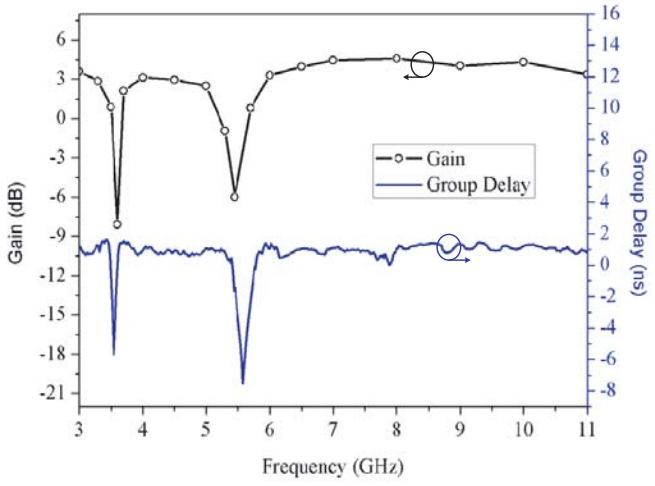

Figure 26. Measured peak gains and group delay of the proposed antenna.

the vicinity of 3.5 and 5.5 GHz. Outside the notched bands, antenna gains with a variation of less than 3 dB is achieved, indicating stable gain performance across the operating band. To analyze the signal dispersion, the group delay is also measured between two identical antennas in the face-to-face orientation, with a distance of 0.30 m between them, and the group delay fluctuates within 2 ns except the notched bands, showing stable group delay in the operating frequencies.

5. CONCLUSION

This study presents a novel compact microstrip-fed printed monopole antenna with dual band-notched characteristic for UWB applications. Assisted with symmetrical open-circuited stubs, the impedance matching at low frequencies can be greatly improved, thus resulting in a UWB performance. A novel modified CLL resonator is introduced to realize the dual band-notched characteristic in this paper. Both the desired notched bands can be achieved by adjusting the parameters of the resonators. Furthermore, employing the resonators in the vicinity of the feed line does not perturb the radiating behavior. The compact size, simple structure, and excellent performance make the proposed antenna a good candidate for UWB applications.

REFERENCES

1. Federal Communications Commission, Washington, DC, "Revision of part 15 of the commission's rules regarding ultra-wideband transmission systems, first note and order," ET-Docket 98-153, 2002.
2. Zhang, S.-M., F.-S. Zhang, W.-Z. Li, T. Quan, and H.-Y. Wu, "A compact UWB monopole antenna with WiMAX and WLAN band rejections," *Progress In Electromagnetics Research Letters*, Vol. 31, 159–168, 2012.
3. Kang, X., H. Zhang, Z. Li, Q.-X. Guo, X. Zhang, J.-H. Wang, and Y. L. Yang, "A band-notched UWB printed elliptical-ring monopole antenna," *Progress In Electromagnetics Research C*, Vol. 35, 23–33, 2013.
4. Chu, Q. X. and Y. Y. Yang, "3.5/5.5 GHz dual band-notch ultra-wide-band antenna," *Electronics Letters*, Vol. 44, 172–174, Jan. 2008.
5. Li, C.-M. and L.-H. Ye, "Improved dual band-notched UWB slot antenna with controllable notched bandwidths," *Progress In Electromagnetics Research*, Vol. 115, 477–493, 2011.
6. Nguyen, D. T., D. H. Lee, and H. C. Park, "Very compact printed triple band-notched UWB antenna with quarter-wavelength slots," *IEEE Antennas and Wireless Propagation Letters*, Vol. 11, 411–414, 2012.
7. Tilanthe, P., P. C. Sharma, and T. K. Bandopadhyay, "A monopole microstrip antenna with enhanced dual band rejection for UWB applications," *Progress In Electromagnetics Research B*, Vol. 38, 315–331, 2012.
8. Zhu, F., S. Gao, A. T. S. Ho, C. H. See, R. A. Abd-Alhameed, J. Li, and J. Xu, "Design and analysis of planar ultra-wideband antenna with dual band-notched function," *Progress In Electromagnetics Research*, Vol. 127, 523–536, 2012.
9. Emadian, R., M. Mirmozafari, C. Ghobadi, and J. Nourinia, "Bandwidth enhancement of dual band-notched circle-like slot antenna," *Electronics Letters*, Vol. 48, 356–357, Mar. 2012.
10. Zhou, H.-J., B.-H. Sun, Q.-Z. Liu, and J.-Y. Deng, "Implementation and investigation of U-shaped aperture UWB antenna with dual band-notched characteristics," *Electronics Letters*, Vol. 44, 1387–1388, Nov. 2008.
11. Gong, J.-G., Y.-C. Jiao, Q. Li, Y.-B. Yang, and S. Gai, "Dual band-notched UWB antenna with parasitic elliptical radiation patch," *International Conference on Microwave and Millimeter Wave Technology (ICMMT)*, 420–423, Chengdu, China, May 8–11, 2010.
12. Li, W. T., Y. Q. Hei, W. Feng, and X. W. Shi, "Planar antenna for 3G/Bluetooth/WiMAX and UWB applications with dual band-notched characteristics," *IEEE Antennas and Wireless Propagation Letters*, Vol. 11, 61–64, 2012.

13. Elboushi, A., O. M. Ahmed, A. R. Sebak, and T. A. Denidni, "Study of elliptical slot UWB antennas with a 5.0–6.0 GHz band-notch capability," *Progress In Electromagnetics Research C*, Vol. 16, 207–222, 2010.
14. Hong, C.-Y., C.-W. Ling, I-Y. Tarn, and S.-J. Chung, "Design of a planar ultrawideband antenna with a new band-notch structure," *IEEE Transactions on Antennas and Propagation*, Vol. 55, No. 12, 3391–3397, Dec. 2007.
15. Lin, C.-C., P. Jin, and R. W. Ziolkowski, "Single, dual and tri-band-notched ultrawideband (UWB) antennas using capacitively loaded loop (CLL) resonators," *IEEE Transactions on Antennas and Propagation*, Vol. 60, No. 1, 102–109, Jan. 2012.
16. Tang, W. and J.-S. Hong, "Coupled stepped-impedance-resonator bandstop filter," *IET Microwaves, Antennas & Propagation*, Vol. 4, 1283–1289, 2010.